Carbohydrate Polymers 164 (2017) 83–91

Contents lists available at ScienceDirect

Carbohydrate Polymers

journal homepage: www.elsevier.com/locate/carbpol

Hydrophobic edible films made up of tomato cutin and pectin

Anny Manrich[a,*], Francys K.V. Moreira[b], Caio G. Otoni[a,b], Marcos V. Lorevice[a,c], Maria A. Martins[a], Luiz H.C. Mattoso[a]

[a] National Nanotechnology Laboratory for Agribusiness, Embrapa Instrumentation – Rua XV de Novembro, 1452, São Carlos, SP 13560-970, Brazil
[b] Department of Materials Engineering, Federal University of São Carlos – Rodovia Washington Luís, km 235, São Carlos, SP 13566-905, Brazil
[c] PPGQ, Department of Chemistry, Federal University of São Carlos – Rodovia Washington Luís, km 235, São Carlos, SP 13566-905, Brazil

ARTICLE INFO

Article history:
Received 19 October 2016
Received in revised form 20 January 2017
Accepted 20 January 2017
Available online 22 January 2017

Keywords:
Biopolymer
Edible film
Hydrophobicity
Water resistance
Water affinity
Bio-based packaging

ABSTRACT

Cutin is the biopolyester that protects the extracellular layer of terrestrial plants against dehydration and environmental stresses. In this work, cutin was extracted from tomato processing waste and cast into edible films having pectin as a binding agent. The influences of cutin/pectin ratio (50/50 and 25/75), film-forming suspension pH, and casting method on phase dispersion, water resistance and affinity, and thermal and mechanical properties of films were investigated. Dynamic light scattering and scanning electron microscopy revealed that cutin phase aggregation was reduced by simply increasing pH. The 50/50 films obtained by casting neutral-pH suspensions presented uniform cutin dispersion within the pectin matrix. Consequently, these films exhibited lower water uptake and solubility than their acidic counterparts. The cutin/pectin films developed here were shown to mimic tomato peel itself with respect to mechanical strength and thermal stability. Such behavior was found to be virtually independent of pH and casting method.

1. Introduction

Ultimate packaging materials are urged to meet aesthetic, barrier, and mechanical requirements for food applications. In addition to these desirable characteristics, an ideal packaging would be originated from inexpensive, renewable raw materials. For decades, bio-based packaging materials have been developed by means of incorporating selected components into film packaging models. However, developing materials made up only of biomolecules is challenging and has brought scientists of diverse areas to integrate knowledge and approaches in order to meet those expectations as well as sufficiently assign the market for edible films and coatings (Cerqueira, Teixeira, & Vicente, 2016).

Edible films feature the capability of being eaten alongside the food they contain. These materials can provide food products with improved nutritional and sensory quality as well as extended shelf life by acting as a physical barrier for gases and water vapor, thereby preserving food color, texture, and moisture (Giosafatto et al., 2014a, 2014b). Edible films may also be incorporated with functional additives, such as antioxidants, antimicrobials, and vitamins (Saha et al., 2016).

Edible films based on proteins and/or polysaccharides may achieve exceptional properties and even replace packaging materials from petrochemical sources, even though the formers are rarely waterproof. An innovative food wrap based on casein and citrus pectin developed by Bonnaillie, Zhang, Akkurt, Yam, and Tomasula (2014) could efficiently prevent food spoilage due to its high oxygen barrier. This material is being considered by some companies for commercial applications, according to CBC News (2016). Improving water resistance properties of edible films has been of relevance to numerous researches. Rhim (2004) prepared water-resistant alginate films through crosslinking in Ca^{2+} solutions. Di Pierro, Sorrentino, Mariniello, Giosafatto, and Porta (2011) reported another example of active barrier films. These authors developed a chitosan/whey protein film capable of extending the shelf life of ricotta cheese through a controlled water vapor permeability (WVP). Decreased WVP as well as improved mechanical strength were also observed by Chambi and Grosso (2006), who investigated casein/gelatin films crosslinked with transglutaminase. Significantly improved barriers against CO_2 and O_2 as well as suitable mechanical properties were achieved by films prepared with citrus pectin and transglutaminase-crosslinked protein phaseolin. These properties were maintained even throughout cold storage, demonstrating that such films can be used to substitute packaging for refrigerated foods (Giosafatto et al., 2014a, 2014b).

* Corresponding author.
E-mail addresses: anny.manrich@gmail.com, anny@daad-alumni.de (A. Manrich), moreira.fkv@gmail.com (F.K.V. Moreira), cgotoni@gmail.com (C.G. Otoni), marcos.lorevice@gmail.com (M.V. Lorevice), maria-alice.martins@embrapa.br (M.A. Martins), luiz.mattoso@embrapa.br (L.H.C. Mattoso).

http://dx.doi.org/10.1016/j.carbpol.2017.01.075
0144-8617/

Hydrophobic compounds (*e.g.*, grape pomace-extracted oils and waxes) have postponed the solubilization of chitosan films in water (Ferreira, Nunes, Castro, Ferreira, & Coimbra, 2014). Other sources of hydrophobic compounds for application in edible films include biopolyesters such as suberin and cutin, which act as protective barriers to plant cells. Garcia et al. (2014) successfully performed *ex situ* reconstitution of suberin films with interesting barrier properties. Suberin is a polymer that comprises aromatic and polyester domains and that plays a barrier role in underground parts, wound surfaces, and a variety of internal organs of plants (Kolattukudy, 1980). It is highly abundant in cork (Garcia et al., 2014) and bark (Heinämäki et al., 2015). Cutin, on the other hand, may be extracted from tomato processing waste (tomato peel, particularly). According to FAO, 38 million tons of tomato processing waste were produced worldwide in 2014, out of which *ca.* 380,000 t consisted of tomato peels.

Cutin is a biopolyester that features a high-molecular weight (M_w) lipid polymer matrix, which in turn is consisted of hydroxylated, epoxy-hydroxylated, crosslinked, and esterified C_{16} and C_{18} fatty acids covered with a mixture of long-chain aliphatic compounds (*e.g.*, waxes). Cutin is found in extracellular membranes of higher plants. This protective, insoluble barrier prevents plants from water loss and biological attack (Järvinen, Kaimainen, & Kallio, 2010; Kolattukudy, 1980; López-Casado, Matas, Domínguez, Cuartero, & Heredia, 2007). Cutin extracted from different plants has been extensively characterized (Benitez, Matas, & Heredia, 2004; Heredia, 2003; Järvinen et al., 2010; Kolattukudy, 1980; Petracek & Bukovac, 1995).

Cutin is highly lipophilic, but it is not expected to form tough, free-standing films. Such shortcoming of cutin may be overcome by the addition of pectin - a water soluble polysaccharide - which is largely known for its excellent film-forming properties (Espitia, Du, Avena-Bustillos, Soares, & McHugh, 2014). In this study, pectin was added to tomato peel-extracted cutin in order to produce edible films. Preliminary experiments have shown that blending cutin and pectin leads to undesirable phase separation (Fig. S1). Two strategies were then adopted to obtain edible films featuring uniform phase morphology: casting them in a faster fashion through continuous casting or producing kinetically stable film-forming suspensions (FFSs) by changing the FFS pH. The cutin/pectin films were characterized by infrared spectroscopy, scanning electron microscopy, contact angle measurements, water uptake and solubility determinations, tensile tests, and thermogravimetry.

2. Experimental

2.1. Cutin extraction

Tomato (*Solanum lycopersicum*, variety Carmen) peels (TmPs) were manually separated from seeds and pulp after blanching ripe tomatoes in boiling water for 60 s. Cutin was extracted in accordance with the methodology proposed by Cicognini (2015). Briefly, dried TmPs were immersed into 3 wt.% NaOH solution (pH *ca.* 14) and autoclaved at 121 °C for 120 min. The liquid phase was collected by filtration and then acidified with 6 mol L^{-1} HCl solution till pH 5–6 to precipitate cutin. Suspensions were centrifuged for 15 min at 8650*g*, washed twice with distilled water, centrifuged likewise, and freeze-dried to recover cutin. The extraction yield was 25 ± 2%.

2.2. Preparation of cutin/pectin films

2.2.1. Film-forming suspension

Cutin was added to ultrapure water – ρ = 18.2 MΩ cm, obtained with a Milli-Q (Barnstead Nanopure Diamond) system – at a concentration of 10% (w/v) and dispersed by 4 successive 30-s ultrasound cycles using a 3.2-mm-diameter tapered microtip (model 101-148-062) at 10% amplitude attached to a Branson Ultrasonics Sonifier™ S-450 digital ultrasonic cell disruptor/homogenizer. Low-methoxyl pectin (M_w = 170,000 g mol^{-1}, CPKelco, Brazil) was dissolved in ultrapure water at 25 °C using a mechanical stirrer to obtain a 6% (w/v) solution. This aqueous pectin solution (pH *ca.* 3.2) was added to the cutin suspension at proper amounts to produce FFSs comprising cutin/pectin weight ratios equal to 25/75 and 50/50. Acidic – original pH of pectin solution in water, *i.e.*, 3.2 – and neutral FFSs were produced, the latter being obtained by adding 0.5 mol L^{-1} of NH_4OH dropwise to the pectin solution until pH 7.0 was reached. FFSs were then vacuum degassed for 30 min and gently stirred in a magnetic stirrer. The solid contents in all FFSs were the same – *i.e.*, 3% (w/v) – regardless of the composition.

2.2.2. Bench casting

Twenty grams of FFS was spread onto 90-mm-diameter glass Petri dishes (0.0092 g solids cm^{-2} casting surface) and allowed to dry overnight at 45 °C. Neat pectin films were prepared likewise for comparison purposes.

2.2.3. Continuous casting

Acidic FFSs were also dried in a KTF-S labcoater casting machine (Werner Mathis AG, Switzerland) running at 120 °C and with a conveyor speed of 0.12 m min^{-1}. The wet layer thickness was set to 1.5 mm. Again, neat pectin films were prepared at the same conditions in order to allow comparison. All samples were conditioned in a desiccator at 52 ± 3% RH and 25 ± 2 °C for at least 48 h prior to testing.

2.3. Attenuated total reflection Fourier transform infrared spectroscopy (ATR-FTIR)

FTIR measurements were carried out on a FT-NIR VERTEX spectrometer (Bruker, Germany) operating in attenuated total reflection (ATR) mode. ATR-FTIR spectra were recorded with a 100-μm-wide Ge crystal at wavenumbers ranging from 600 to 4000 cm^{-1} using an accumulation of 32 scans and resolution of 1 cm^{-1}.

2.4. Dynamic light scattering (DLS)/electrophoretic mobility determinations

Hydrodynamic zeta-average diameter (Z_{ave}) of TmP-cutin was determined at 25 °C by DLS using a Zetasizer Nano Series (Malvern Instruments Inc., Worcestershire, UK) at pH ranging from 2.0 to 10.0. Zeta potential (ζ) determinations were performed simultaneously. Ultrapure water was used as a dispersant to avoid multiple scattering effects and inter droplet interactions.

2.5. Scanning electron microscopy (SEM)

TmP and cutin/pectin films were imaged on a JEOL microscope. Samples were first cryo-fractured in liquid N_2 and then fixed onto 90° specimen mounts. Once coated by a *ca.* 5-nm-thick gold layer in an argon atmosphere, samples were analyzed using an accelerating voltage of 5 kV and a working distance of *ca.* 10 mm. All SEM images were taken using the secondary electron mode.

2.6. Contact angle measurements

Contact angle was determined in a CAM 101 Optical Contact Angle Meter (KSV Instruments) equipped with a CCD KSV-5000 digital camera. For each measurement, 5 μL of ultrapure water was dropped onto film surface and 100 images were automatically recorded within an experimental time of 60 s using the KSV CAM2008 software. Upper and lower surfaces of each sample were

assayed separately. Contact angle determinations were performed with 5 replicates as per ASTM D5725-99 (2008). Contact angle was calculated by averaging the compiled angle values at selected check points (*i.e.*, 0.2, 1.5, and 10.5 s).

2.7. Solubility tests

The percentage solubility of cutin/pectin films in water was measured in accordance with OECD guidelines (OECD, 2017). Samples ($20 \times 20\ mm^2$) were conditioned at 50% RH for at least 48 h and then immersed in 40 mL of ultrapure water, where they were gently stirred at 25 °C. Supernatant aliquots were analyzed periodically on a RX-5000CX Atago digital refractometer for soluble solid content (°Brix) determination using sucrose as an internal calibration standard. Water solubility (S_w) was calculated as $S_w\ (\%) = (c_t/c_\infty) \cdot 100$, where c_t and c_∞ are the concentrations of solubilized film at a time t and maximum film concentration at equilibrium, respectively. Solubility tests were performed in triplicate.

2.8. Water uptake

Water uptake was measured gravimetrically in triplicate following the methodology proposed by Sartori and Menegalli (2016) with slight modifications. Samples were cut into 20-mm-sided squares, dried at 110 °C for 48 h, conditioned at 23 ± 2 °C into a desiccator previously equilibrated at 50% RH with a saturated $Mg(NO_3)_2$ solution, and then weighed to the nearest 0.0001 g every 15 min (at the beginning of the experiment) and every 60 min until 700 min. Water uptake was calculated as w_u ($g_{water}\ g_{film}^{-1}$) = $(m_f - m_o)/m_o$, where m_f and m_o are the masses of swollen and dried films, respectively.

2.9. Thermogravimetry

Thermogravimetric (TG) and differential TG (DTG) curves were recorded on a TGA Q500 thermal analyzer (TA Instruments Inc., New Castle, USA). Samples were heated up to 800 °C at a heating rate of 10 °C min^{-1} in a synthetic air atmosphere (80% N_2 and 20% O_2) flowing at 60 mL min^{-1}.

2.10. Mechanical tests

Elastic modulus (GPa), tensile strength (MPa), and elongation at break (%) were measured at 25 °C in a DMA Q800 V7.0 equipment (TA Instruments Inc.) using an 18 N load cell. Tension film clamp was used to stretch rectangular specimen strips ($55 \times 5\ mm^2$) at a strain rate of 0.1% min^{-1}. Five replicates were performed to define the average tensile properties of each sample. Thickness (t) values of each film had been previously measured in triplicate using an IP 65 Coolant Proof digital micrometer (Mitutoyo Manufacturing, Japan).

2.11. Statistical analysis

One-way analysis of variance (ANOVA) was applied to the data. Mean values were compared using Tukey's test at a confidence level of 95% ($p < 0.05$). All statistical calculi were performed in the Origin software, version 6.0 (OriginLab, Northampton, USA).

3. Results and discussion

3.1. Characterization of TmP-cutin

The external surfaces of TmP and cutin extracted from TmP (TmP-cutin) were examined by ATR-FTIR (Fig. 1a). The cutin fingerprint represented by the intense vibration ester (–COOR) band

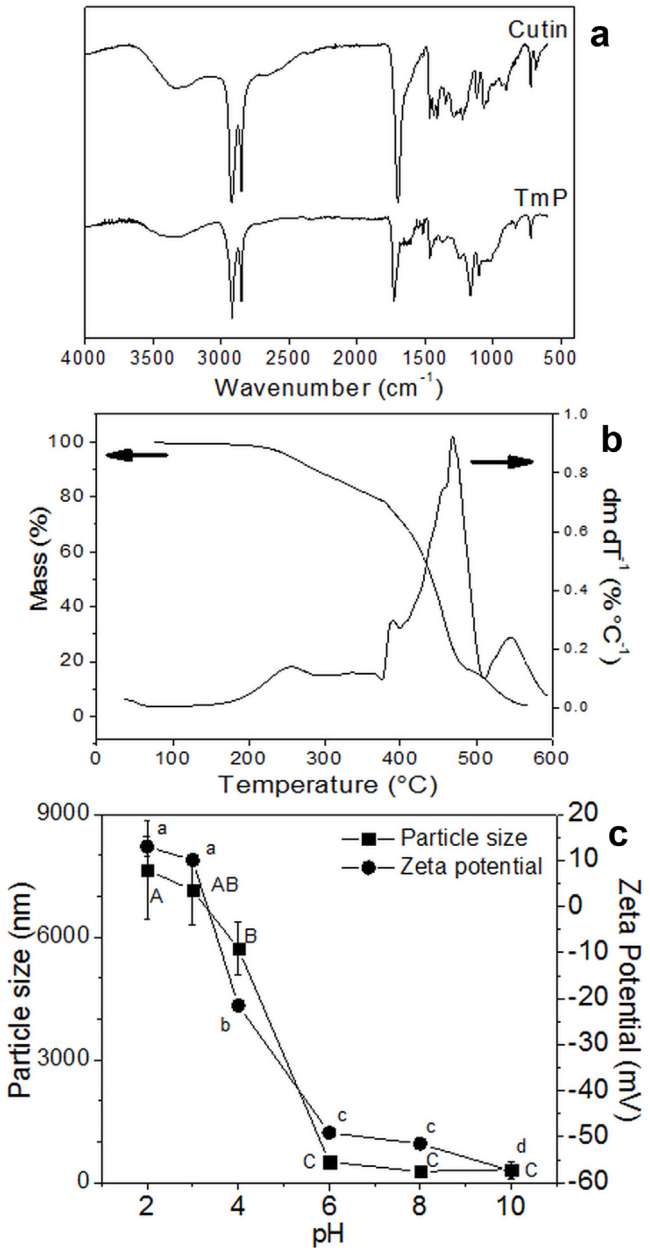

Fig. 1. (a) Normalized ATR-FTIR spectra of untreated tomato peel (TmP) and cutin extracted from TmP (TmP-cutin); (b) Thermogravimetric (TG) and differential TG (DTG) curves of TmP-cutin; (c) Average hydrodynamic size (■) and zeta potential (●) values of TmP-cutin dispersed in ultrapure water at different pH values (different lowercase and uppercase letters indicate significantly different zeta potential and particle size values, respectively, as indicated by Tukey's test – $p < 0.05$).

at 1730 cm^{-1} as well as the vibration —CH, $—CH_2$, and $—CH_3$ bands related to alkane saturation at 2950 and 2850 cm^{-1} are noticeable in the spectra. Some differences are evident in the fingerprint region (1500–600 cm^{-1}) when comparing the acquired spectra. The additional bands between 1250 and 970 cm^{-1} in the TmP spectrum denote the deformation vibrations of the C—OH groups of carbohydrates, whereas the strong peaks at 1165 and 1102 cm^{-1} relate to the stretching vibrations of the C—O of alcohols (Galat, 1980). In the TmP-cutin spectrum, the presence of absorption bands from 1630 to 500 cm^{-1} and from 900 to 800 cm^{-1} are attributed to functional or structural phenolic and flavonoid groups, which have been described in the cutin of ripe tomato fruits (Benitez et al., 2004). This confirms that cutin was efficiently extracted from TmP (Benitez et al., 2004; Domínguez, Cuartero, & Heredia,

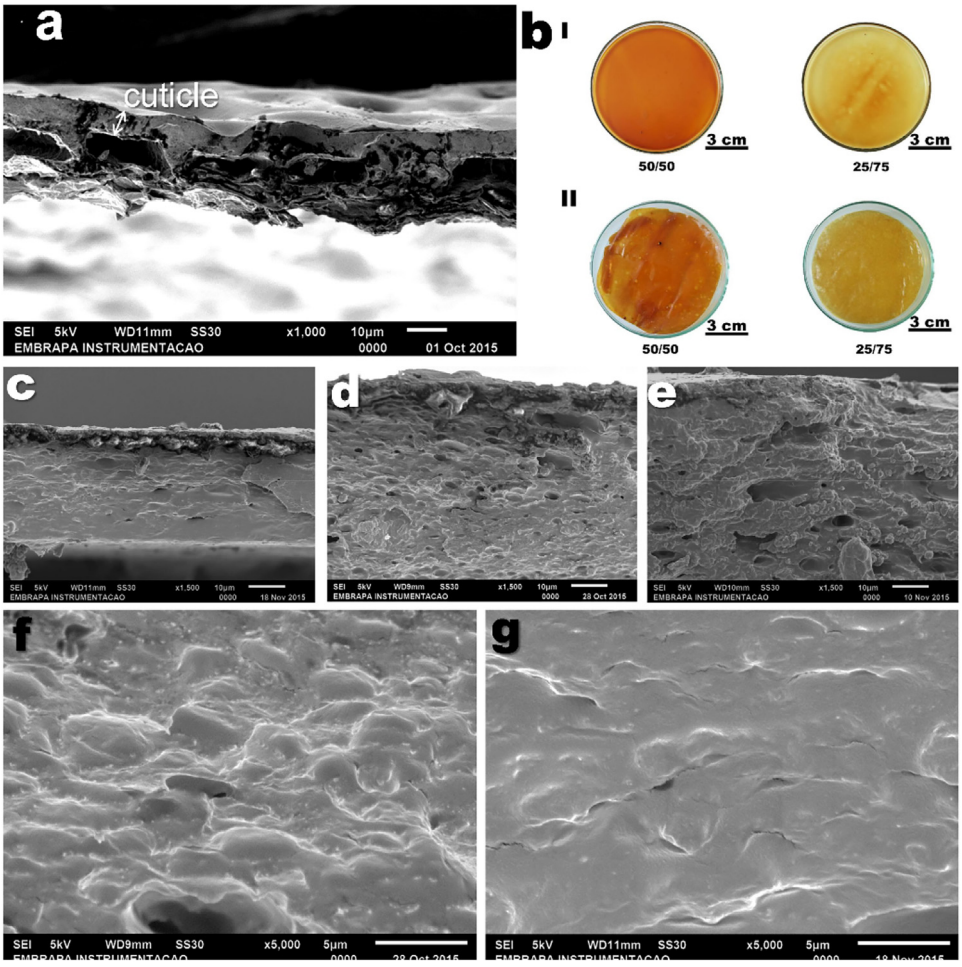

Fig. 2. Cross-sectional scanning electron microscopy (SEM) micrographs of untreated tomato peel (TmP) (a); Visual aspect of 50/50 and 25/75 cutin/pectin films produced by bench (I) and continuous casting (II) (b); Cross-sectional SEM micrographs of 50/50 neutral-cutin/pectin film produced by bench casting (c and g) as well as of 50/50 acidic-cutin/pectin film produced by bench (d and f) and continuous casting (e).

2011; Heredia-Guerrero, Heredia, García-Segura, & Benítez, 2009). TG/DTG curves (Fig. 1b) provide further compositional information on TmP-cutin.

TmP-cutin was thermally stable up to *ca.* 200 °C. From this temperature on, three mass loss steps were observed, which presented maximum mass loss rates at *ca.* 390, 469, and 546 °C. Such a high thermal stability was attributed to the presence of three-dimensional, heavily crosslinked structures (Ferreira et al., 2013). Chaudhari and Singhal (2015) reported similar results. These authors found 200 °C to be the thermal stability threshold of cutin extracted from watermelon peels. The same authors observed a slight mass loss stage at lower temperatures (maximum rate at *ca.* 68 °C), which has been attributed to the physical desorption of water (Chaudhari & Singhal, 2015). This moisture loss was not observed in the TmP-cutin investigated here, corroborating its hydrophobic aspect. Fig. 1b also reveals that TmP-cutin can be processed to obtain films up to 200 °C without degradation.

Fig. 1c shows the evolution of hydrodynamic size and zeta potential of TmP-cutin in aqueous suspensions having different pH values. In acidic media, cutin molecules occur as micrometric agglomerates with slightly positive surface charge density. At the original pH of pectin solution (*i.e.*, 3.2), the Z_{ave} diameter of cutin agglomerates was approximately 7.1 µm. The variation of pH between 2.0 and 3.5 significantly influenced neither Z_{ave} diameter nor zeta potential ($p > 0.05$). Conversely, increasing the pH of the TmP-cutin suspensions until pH 6.0 resulted in a sharp reduction in Z_{ave} diameter towards the nanoscale. Cutin agglomerate sizes achieved a plateau at which the Z_{ave} diameters were unchanged ($p > 0.05$) for pH values higher than 6.0. It was verified that zeta potential also became strongly negative with increasing pH, reaching −55 mV at pH 10.0.

From DLS and zeta potential outcomes, we hypothesized that the coalescence of TmP-cutin throughout the casting process could be prevented by simply increasing FFS pH. The kinetic phase stability is indicated by highly negative zeta potentials as well as small hydrodynamic sizes at pH higher than 6.0. Fig. 1c suggests that a high mixture level between cutin and pectin can be attained when cutin/pectin films are produced from neutral FFSs rather than from their acidic counterparts. This strategy was expected to prevent undesirable phase separation between the immiscible macromolecules (Fig. S2).

3.2. Characterization of cutin/pectin films

3.2.1. Morphological aspects

Fig. 2a displays a SEM micrograph of untreated TmP cross-section in which the typical lamellar ultra-structure is recognized (Kolattukudy, 1980). Morphological evidence of cuticle in TmP is indicated by the uniform, smooth layer that covers the ellipsoidal cells of TmP epidermis (Kolattukudy, 1980; Martin & Rose, 2014). The average cutin density and cuticle thickness of tomato have been reported to be 717 µg cm^{-2} and 6–12 µm, respectively (Bargel &

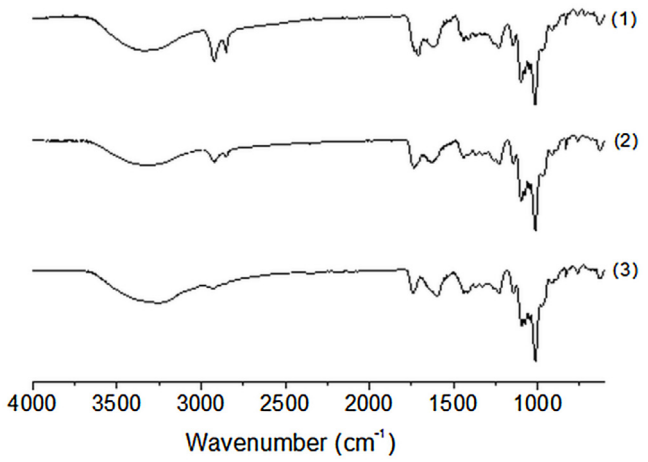

Fig. 3. Normalized ATR-FTIR spectra of cutin/pectin films comprising cutin/pectin ratios of (1) 50/50 and (2) 25/75. The spectrum of a neat pectin film (3) was included as reference. Films were produced through bench casting of acidic (pH = 3.2) film-forming suspensions. This behavior is representative of the other compositions studied here, which are available as supplementary material.

Neinhuis, 2005; Martin & Rose, 2014). The thickness of the cuticle displayed in Fig. 1a was 7.6 ± 1.1 μm.

Using pectin as a binding agent enabled casting of TmP-cutin into films with distinct homogeneity and color (Fig. 2b). The morphology of the TmP-cutin/pectin films was found to be particularly dependent on FFS pH (Fig. 2c–g). While 50/50 neutral-cutin/pectin films exhibited a compact and rather homogeneous structure (Fig. 2c), the analogous films produced from acidic FFSs clearly displayed biphasic morphology regardless of the casting method (Fig. 2d–e). The cutin-rich phase is identified in Fig. 2e and f as globular domains with size varying between 1.7 and 4.8 μm. These values are in good agreement with the hydrodynamic cutin sizes reported in Fig. 1c. Conversely, little morphological information of round cutin domains is seen in Fig. 2g, probably due to their nanometric size at pH higher than 6. Changing pH was revealed to facilitate cutin dispersion, leading to an enhanced continuity of this lipophilic biopolyester within film matrices.

3.2.2. Structural aspects

Normalized ATR-FTIR spectra registered on areas of approximately 300 μm^2 from distinct surfaces of cutin/pectin films are shown in Fig. 3.

The intensity of bands related to C—H stretching at 2950 and 2850 cm^{-1} increased with increasing cutin/pectin ratios. Also, the intensity of peaks that are typical of carbohydrates between 1200 and 1500 cm^{-1} decreased markedly upon cutin/pectin ratio increase. The band at 1750 cm^{-1} corresponding to —C=O stretching vibration of cutin is noticeable in the 50/50 cutin/pectin film spectrum. Normalized ATR-FTIR spectra recorded on air- and substrate-contacting surfaces showed no significant numerically differences in peak values. The ATR-FTIR spectra of films from both acidic and neutral FFSs (Fig. S1) support that there was no phase separation in cutin/pectin films, nevertheless SEM micrographs (Fig. 2) revealed their structural differences.

3.2.3. Water affinity aspects

The hydrophobicity of the cutin/pectin films was evaluated by contact angle measurements. Fig. 4 shows average contact angle values for 50/50 and 25/75 cutin/pectin films produced through bench casting neutral and acidic FFSs as well as by continuously casting acidic FFSs. The hydrophobic effect attributed to cutin was reflected on all cutin/pectin films and is undoubtedly revealed if contact angle values of neat pectin films are observed and contrasted to those of films added by TmP-cutin.

Contact angle is an evaluation of the affinity between the solvent and the surface of the material. Therefore, it is expected that higher TmP cutin contents in the FFS lead to higher contact angles between water drops and film surfaces, being hydrophobicity driven by film composition (Pereda, Amica, & Marcovich, 2012). Ferreira et al. (2014) verified increased contact angle values when higher amounts of hydrophobic compounds (grape pomace wax and oil) were incorporated into chitosan films, whereas decreased values were observed when a polar (polysaccharide-based) extract was added. Similar results were reported by Ojagh, Rezaei, Razavi, and Hosseini (2010), when casting chitosan films incorporated by cinnamon essential oil. Slightly different hydrophobic characters were observed among upper (*i.e.*, air-contacting) and lower (*i.e.*, substrate-contacting) film surfaces, the former presenting a tendency of being more hydrophobic than the latter. This behavior was comparable to the effect of the biopolyester on untreated TmP itself, in which the inner (*i.e.*, pulp-contacting) surface (contact angle = 64 ± 4 °) was more hydrophilic than the outer (*i.e.*, air-contacting) one (contact angle = 84 ± 4 °). Besides surface composition, the outmost (monolayer) surface structure affects the wettability properties of the film, whereas a dense external structure contributes for higher contact angle values (Basiak, Debeaufort, & Lenart, 2015).

No significant ($p > 0.05$) contact angle differences were noticed between 50/50 and 25/75 cutin/pectin films, regardless of casting method. On the other hand, cutin/pectin films originated from neutral FFSs were shown to be more hydrophobic than the analogous films produced from acidic FFSs. These results are in line with SEM and ATR-FTIR observations, which revealed a homogeneous distribution and a uniform cutin dispersion within film matrices. This led to the large contact angle values found at the surfaces of both films. A similar behavior was observed for cutin/pectin films prepared by continuous casting. The fast solvent removal rate of the continuous process may have lessened phase separation effects in cutin/pectin films, thereby imparting high hydrophobicity to films, particularly those containing 50 wt.% cutin.

The water uptake behavior of the hydrophobic cutin/pectin films is shown in Fig. 5.

It can be observed that high cutin/pectin ratio is a determining factor on water uptake. The 50/50 cutin/pectin films absorbed a considerably smaller amount of water over time when compared with the neat pectin matrix, which is highly hygroscopic. The difference between the water uptake behavior of cutin/pectin films prepared from acidic (Fig. 5a) and neutral (Fig. 5b) FFSs as well as continuously cast acidic FFSs (Fig. 5c) is obvious. Unlike in acidic-cutin/pectin films, a high dispersion of cutin within the matrices of neutral-cutin/pectin and acidic/continuously cast-cutin/pectin was attained. Thus, water uptake was reduced by the uniform occurrence of such biopolyester featuring low water affinity throughout the film structure. Indeed, the increase in film hydrophobicity resulted in increased water resistance (Chambi & Grosso, 2006). Moreover, it is worth pointing out that the water uptake behavior of neat pectin film was significantly ($p > 0.05$) affected neither by FFS pH nor by casting method. This confirms that the reduced water uptake of cutin/pectin films, evidenced by comparing Fig. 5b and c with Fig. 5a was due to the well-dispersed hydrophobic cutin phase. These results are in agreement with those reported by other authors (Sartori & Menegalli, 2016).

Fig. 6 displays the evolution of water solubility (S_w) over time in hydrophobic cutin/pectin films. S_w outcome of neat pectin matrix is also reported.

Neat pectin films were entirely solubilized in water (*i.e.*, S_w = 95–99%) within 5 h. This confirms that there was no influence of pH and casting method on the water barrier properties of pectin

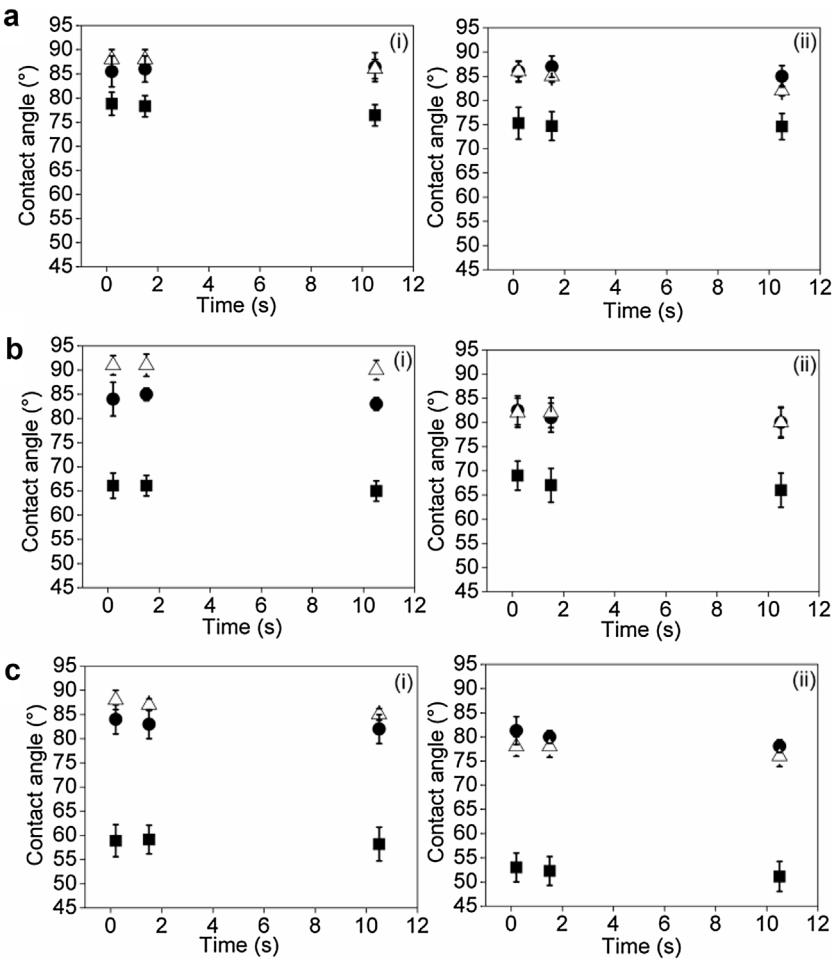

Fig. 4. Contact angle values (i: air-contacting surface; ii: substrate-contacting surface) of (a) neutral cutin/pectin films, (b) acidic cutin/pectin films, and (c) acidic/continuously cast cutin/pectin films comprising cutin/pectin weight ratios of (△) 50/50 and (●) 25/75. Data of neat pectin films (■) were included in all sets for comparison purposes.

films. On the other hand, the presence of cutin clearly affected the solubilization rate of the films, regardless of the cutin/pectin ratio.

The S_w values were noticeably reduced in the 50/50 cutin/pectin films. For instance, while neat pectin and 25/75 cutin/pectin films reached S_w *ca.* 20% within 1 h, 50/50 cutin/pectin films required a two-fold time to achieve the same solubilization extent. Moreover, considerably reduced S_w values were observed for the 50/50 neutral cutin/pectin and acidic/continuously cast cutin/pectin films (Fig. 6b and c, respectively) when compared with those of 50/50 acidic cutin/pectin films (Fig. 6a). This observation supports the hypothesis of achieving uniform dispersions of the lipophilic cutin phase within the edible film structure either through the bench casting of neutral FFSs or by fast drying acidic FFSs. In both cases, cutin coalescence is suppressed. The smaller solubilization rate of the 50/50 cutin/pectin films reveals the efficiency of cutin in forming water-resistant edible films.

Cutin is a polymeric lipid component of hydrophobic layers of plant cell walls, acting as a barrier to permeation of gases, moisture, and solutes (Pollard et al., 2008). The moisture barrier properties, in particular, are due to their remarkably low affinity to water and water vapor. We relied upon these characteristics of cutin to produce cutin/pectin films with reduced water uptake and increased water resistance. Studies with similar purposes have been carried out by adding lipids to improve water resistance of water-soluble films. Sartori and Menegalli (2016) performed water affinity tests on banana starch films containing solid lipid microcapsules. The microcapsules reduced the WVP and water uptake of the films, which was correlated with the low water affinity of the lipid fraction. Acosta, Jiménez, Cháfer, González-Martínez, and Chiralt (2015) also discussed the water affinity in cassava starch/gelatin films incorporated with mono and diglycerides of fatty acids, which decreased the equilibrium moisture in the films and led to materials featuring lower water affinity. Jiménez, Fabra, Talens, and Chiralt (2012) reported decreased moisture contents in corn starch-based films upon the incorporation of palmitic and stearic acids. In addition to the low water affinity of these lipids, the homogeneous distribution of fatty acids within the film matrix reduced water diffusion rates and increased water resistance of the films. Ferreira et al. (2014) reported that the incorporation of grape pomace extract oil into chitosan-based films resulted in films featuring 75% lower water solubility when compared with pure chitosan films. The oil was also responsible for a significant increase (8%) in contact angle values. A similar outcome was observed here. We demonstrated that reduced water uptake was enabled by cutin, which formed water resistant films even when cast with a hydrophilic polysaccharide (*i.e.*, pectin).

3.2.4. *Mechanical aspects*

The cutin/pectin films were further characterized with respect to their mechanical and thermal properties. The results summarized in Table 1 correspond to their thickness (t), tensile strength (σ_T), elastic modulus (E), and elongation at break (ε_B).

Data of untreated TmP and neat pectin films were also reported and showed that cutin/pectin films attained intermediate mechan-

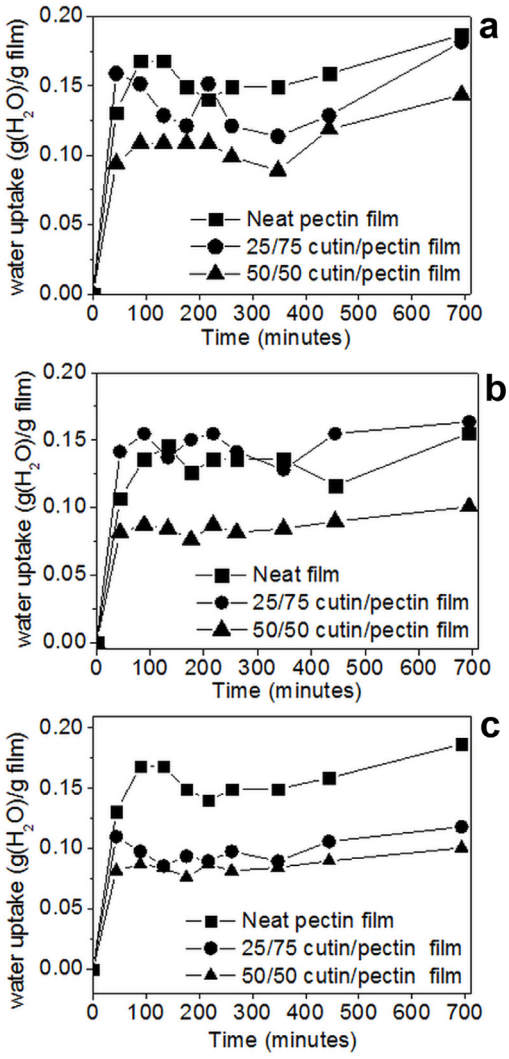

Fig. 5. Water uptake *vs.* time curves for (a) acidic cutin/pectin films, (b) neutral cutin/pectin films, and (c) acidic/continuously cast cutin/pectin films comprising cutin/pectin weight ratios of 50/50 and 25/75.

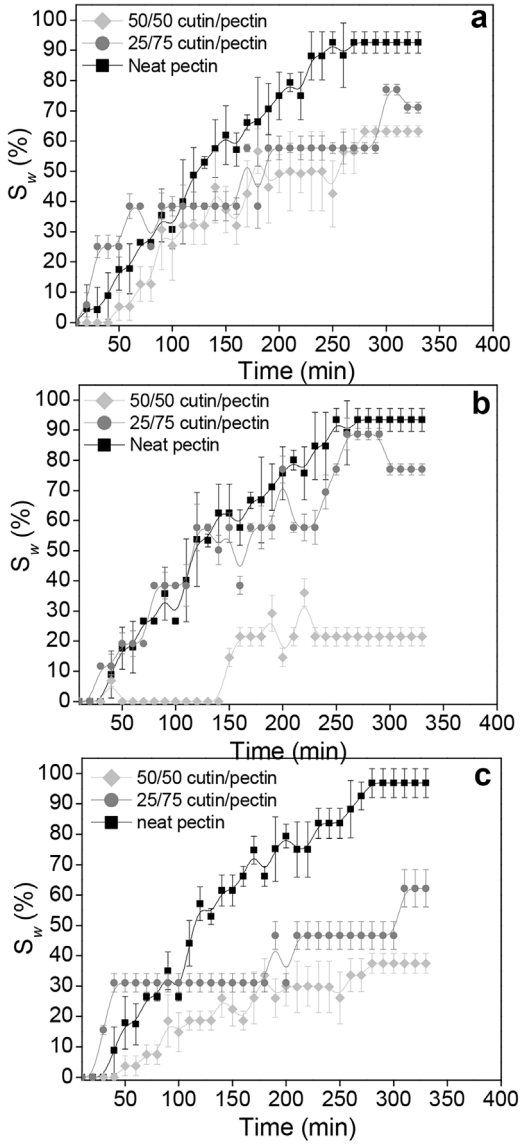

Fig. 6. Solubility (S_w) *vs.* time (a) of acidic, (b) neutral, and (c) acidic/continuously cast pectin films comprising cutin/pectin weight ratios of 0/100 (neat pectin), 50/50, and 25/75.

ical behavior (*i.e.*, between the mechanical attributes of the formers). The average values of σ_T and E of untreated TmP found here were *ca.* 14 MPa and 0.9 GPa, respectively, which are in close agreement with earlier reported data (Domínguez et al., 2011; Hetzroni et al., 2011). This material behaved as an elastic, brittle solid, which is mainly denoted by the low ε_B (Hetzroni, Vana, & Mizrach, 2011; Matas, Cobb, Bartsch, Paolillo, & Niklas, 2004).

Neat pectin films were also rigid, but presented higher mechanical resistance than TmP. Importantly, no significant differences were observed among the σ_T and ε_B values of acidic- and neutral-pectin films ($p > 0.05$). Mechanical properties at fracture of pectin films were also independent on the casting method ($p > 0.05$).

By analyzing the mechanical data of cutin/pectin films (Table 1), it is possible to confirm that the impregnation of cutin into pectin matrix formed water-resistant films with reasonable mechanical strength, particularly considering that cutin itself did not exhibit film-forming ability. For each cutin/pectin weight ratio, the σ_T of the acidic-, neutral-, and acidic/continuously cast-cutin/pectin films were statistically similar to that of untreated TmP ($p > 0.05$).

The E values of cutin/pectin films were two-fold greater than that of TmP ($p < 0.05$). E values increased while ε_B slightly decreased with decreasing cutin/pectin weight ratios. These data resemble the well-known mechanical synergy between the polysaccharide fraction and the cutin matrix in vegetable cuticles, the former accounting for the high E and maximum stress, whereas the latter is responsible for the high extensibility (Domínguez et al., 2011). Tensile properties reveal that cutin/pectin films closely mimic the mechanical behavior of TmP, but alternatively reaching higher stiffness ($p < 0.05$). One can finally notice from Table 1 that hydrophobic cutin/pectin films were also similar to TmP in terms of thickness. Ferreira et al. (2014) described decreased stiffness upon the addition of grape pomace oil into chitosan films. Indeed, the incorporation of grape pomace wax and oil into the films also resulted in lower tensile strength values. The authors stated that this could be explained by structure discontinuities induced by the addition of lipid into the polysaccharide matrix, which resulted in a film structure with lower chain mobility and matrix cohesiveness. On the contrary, it is expected that crosslinking effects, and consequently reduction of discontinuities, of additional hydrophobic compounds into the matrix may lead to improved mechanical properties. This was observed after the incorporation of olive oil into chitosan films (Pereda et al., 2012).

Table 1
Thickness (t), mechanical (σ_T: tensile strength; E: elastic modulus; ε_B: elongation at break), thermal data, and moisture content (MC) of tomato peel, untreated cutin, neat pectin films, and cutin/pectin films.

Sample	T (μm)	σ_T (MPa)	E (GPa)	ε_B (%)	T_{onset} (°C)	T_{max1} (°C)	MC (wt.%)
50/50							
Acidic-cutin/pectin film	52 ± 13^{a}	9.6 ± 2.7^{a}	3.0 ± 0.9^{a}	0.6 ± 0.2^{a}	208	239	2.0
Neutral-cutin/pectin film	58 ± 2^{a}	10.1 ± 4.2^{a}	1.7 ± 0.4^{b}	1.1 ± 0.6^{ab}	210	237	1.6
Acidic/continuously cast-cutin/pectin film	76 ± 4^{b}	9.8 ± 3.9^{a}	1.7 ± 0.3^{b}	0.9 ± 0.3^{a}	219	238	2.1
25/75							
Acidic-cutin/pectin film	31 ± 6^{c}	13.3 ± 1.8^{a}	6.2 ± 0.9^{ec}	0.4 ± 0.1^{a}	204	236	2.9
Neutral-cutin/pectin film	52 ± 15^{a}	13.5 ± 1.8^{a}	5.6 ± 0.8^{c}	0.6 ± 0.2^{a}	217	237	1.8
Acidic/continuously cast-cutin/pectin film	53 ± 3^{a}	14.2 ± 2.7^{a}	3.8 ± 0.7^{a}	0.6 ± 0.1^{a}	219	239	2.2
Neat							
Tomato peel	43 ± 5^{c}	13.6 ± 3.1^{a}	0.9 ± 0.5^{d}	2.0 ± 0.9^{b}	216	256	0.3
Cutin	–	–	–	–	216	468	0.9
Acidic-pectin film	19 ± 6^{d}	29.1 ± 3.5^{b}	3.4 ± 0.5^{a}	1.2 ± 0.3^{ab}	216	239	2.0
Neutral-pectin film	17 ± 2^{d}	36.7 ± 6.9^{b}	7.4 ± 0.3^{e}	0.8 ± 0.5^{a}	203	237	2.1
Acidic/continuously cast-pectin film	40 ± 5^{c}	35.0 ± 6.0^{b}	3.1 ± 0.1^{a}	4.0 ± 1.4^{c}	139	227	2.3

[a-e] Mean values ± standard deviations followed by equal superscript letters within the same column are not different ($p > 0.05$).

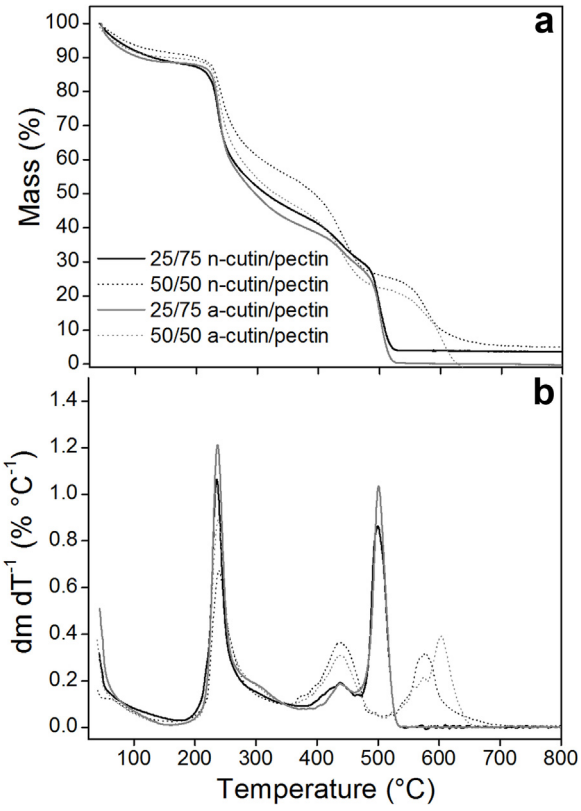

Fig. 7. (a) Thermogravimetric (TG) and (b) differential TG (DTG) curves of cutin/pectin films obtained from bench casting of acidic (a-) and neutral (n-) film-forming suspensions.

3.2.5. Thermal aspects

Representative TG/DTG curves of cutin/pectin films are shown in Fig. 7. Moisture content (MC, wt.%), initial temperature of thermal degradation (T_{onset}) and temperature at first maximum degradation rate (T_{max1}) of all investigated samples are also summarized in Table 1.

Regardless of FFS pH, cutin/pectin films presented four well-defined mass loss stages. The initial stage that appears in all TG curves – up to approximately 150 °C – can be ascribed to elimination of water adsorbed into the film matrix (Monfregola, Bugatti, Amodeo, De Luca, & Vittoria, 2011). It can be observed that the cutin/pectin ratio had a little influence on the T_{onset} values of the films. This parameter corresponds to the onset of thermal degradation of the pectin fraction (Moreira, De Camargo, Marconcini, & Mattoso, 2013), but also to that of neat cutin, as seen in Fig. 1b. The T_{max} related to this step was also independent on cutin/pectin ratio, pH, and casting method (Table 1).

Fig. 7 shows that the intensity of the third mass loss stage at 360–480 °C increased with increasing cutin/pectin ratios, thus being attributed to the cutin fraction of the films. The other thermal degradation stages occurring at higher temperatures (T > 485 °C) represent intricate combustion reactions triggered by oxygen. These steps exhibit a trend with respect to the cutin/pectin ratio, which might be attributed to the ignition of the already degraded cutin/pectin films.

Overall, the data presented in Fig. 7 and Table 1 suggest that FFS pH and casting procedure had a minor influence on the thermal profile of the hydrophobic cutin/pectin films. This was particularly confirmed by the similar mass loss stages of films comprising equal cutin/pectin ratios.

4. Conclusions

Water-resistant edible films derived from the tomato peel-extracted biopolyester cutin were obtained upon its casting in the presence of pectin. Enhanced dispersion of cutin phase within pectin matrix was obtained by modulating the pH of the FFSs towards a neutral condition prior to casting. The effect of lipophilic cutin on the cutin/pectin films was confirmed by contact angle, water uptake, and solubility tests. Edible cutin/pectin films were shown to mimic tomato peel in terms of mechanical strength and thermal stability. Nevertheless, uniform surface hydrophobicity and greater stiffness were observed for cutin/pectin films in relation to that naturally occurring ultrastructure. The properties of the films studied here were found to be virtually independent of pH and casting procedure.

Control over water resistance of edible films is of substantial interest to various applications, including for coating minimally processed fruits, vegetables, and other moist food products. In the present study, cutin-based edible films were confirmed to be slightly affected by moisture. Cutin/pectin films may also be used as water-resistant plastic wraps for short-time applications.

Acknowledgements

We gratefully acknowledge the staff and facilities at Embrapa Instrumentation for the support to this work. We also acknowledge Dr. Marcos D. Ferreira for refractometer analysis. This research was supported by National Network of Laboratories for Nano-

technology (SisNANO), a Ministry of Science, Technology and Innovation (MCTI) program, under contract no. 402287/2013-4. C. G. Otoni thanks São Paulo Research Foundation (FAPESP, grant #2014/23098-9).

Appendix A. Supplementary data

Supplementary data associated with this article can be found, in the online version, at http://dx.doi.org/10.1016/j.carbpol.2017.01.075.

References

Acosta, S., Jiménez, A., Cháfer, M., González-Martínez, C., & Chiralt, A. (2015). Physical properties and stability of starch-gelatin based films as affected by the addition of esters of fatty acids. *Food Hydrocolloids*, *49*, 135–143.

ASTM D5725-99(2008). (2008). *ASTM standard test method for surface wettability and absorbency of sheeted materials using an automated contact angle tester*. West Conshohocken, PA: ASTM International.

Bargel, H., & Neinhuis, C. (2005). Tomato (*Lycopersicon esculentum* Mill.) fruit growth and ripening as related to the biomechanical properties of fruit skin and isolated cuticle. *Journal of Experimental Botany*, *56*, 1049–1060.

Basiak, E., Debeaufort, F., & Lenart, A. (2015). Effect of oil lamination between plasticized starch layers on film properties. *Food Chemistry*, *195*, 56–63.

Benitez, J. J., Matas, A. J., & Heredia, A. (2004). Molecular characterization of the plant biopolyester cutin by AFM and spectroscopic techniques. *Journal of Structural Biology*, *147*, 179–184.

Bonnaillie, L. M., Zhang, H., Akkurt, S., Yam, K. L., & Tomasula, P. M. (2014). Casein films: The effects of formulation, environmental conditions and the addition of citric pectin on the structure and mechanical properties. *Polymers*, *6*, 2018–2036.

CBC News. (2016). Milk protein used to make biodegradable food wrap. Available at www.cbc.ca/news/technology/milk-proetein-film-1.3728398. Posted on 21 st August 2016. Accessed 18 January 2017.

Cerqueira, M. A. P. R., Teixeira, J. A. C., & Vicente, A. A. (2016). Edible packaging today. In M. A. P. R. Cerqueira, R. N. C. Pereira, O. L. S. Ramos, O. L. S. Ramos, & A. A. Vicente (Eds.), *Edible food packaging: Materials and processing technologies* (pp. 1–8). New York: CRC Press.

Chambi, H., & Grosso, C. (2006). Edible films produced with gelatin and casein cross-linked with transglutaminase. *Food Research International*, *39*, 458–466.

Chaudhari, S. A., & Singhal, R. S. (2015). Cutin from watermelon peels: A novel inducer for cutinase production and its physicochemical characterization. *International Journal of Biological Macromolecules*, *79*, 398–404.

Cicognini, T. (2015). Extraction method of a polyester polymer or cutin form the wasted tomato peels and polyester polymer so extracted. International Patent WO2015/028299A1.

Di Pierro, P., Sorrentino, A., Mariniello, L., Valeria, C. L., & Porta, G. R. (2011). Chitosan/whey protein film as active coating to extend Ricotta cheese shelf-life. *LWT–Food Science and Technology*, *44*, 2324–2327.

Domínguez, E., Cuartero, J., & Heredia, A. (2011). An overview on plant cuticle biomechanics. *Plant Science*, *181*, 77–84.

Espitia, P. J. P., Du, W.-X., Avena-Bustillos, R. J., Soares, N. F. F., & McHugh, T. H. (2014). Edible films from pectin: Physical-mechanical and antimicrobial properties–A review. *Food Hydrocolloids*, *35*, 287–296.

Ferreira, R., Garcia, H., Sousa, A. F., Freire, C. S. R., Silvestre, A. J. D., Rebelo, L. P. N., et al. (2013). Isolation of suberin from birch outer bark and cork using ionic liquids: A new source of macromonomers. *Industrial Crops and Products*, *44*, 520–527.

Ferreira, A. S., Nunes, C., Castro, A., Ferreira, P., & Coimbra, M. A. (2014). Influence of grape pomace extract incorporation on chitosan films properties. *Carbohydrate Polymers*, *113*, 490–499.

Galat, A. (1980). Study of the Raman scattering and infrared absorption spectra of branched polysaccharides. *Acta Biochimica Polonica*, *27*, 135–142.

Garcia, H., Ferreira, R., Martins, C., Sousa, A. F., Freire, C. S., Silvestre, A. J., et al. (2014). Ex situ reconstitution of the plant biopolyester suberin as a film. *Biomacromolecules*, *15*, 1806–1813.

Giosafatto, C. V. L., Di Pierro, P., Gunning, A. P., Mackie, A., Porta, R., & Mariniello, L. (2014). Trehalose-containing hydrocolloid edible films prepared in the presence of transglutaminase. *Biopolymers*, *101*, 931–937.

Giosafatto, V. L., Di Pierro, P., Gunning, P., Mackie, A., Porta, R., & Mariniello, L. (2014). Characterization of citrus pectin edible films containing transglutaminase-modified phaseolin C. *Carbohydrate Polymers*, *106*, 200–208.

Heinämäki, J., Halenius, A., Paavo, M., Alakurtti, S., Pitkänen, P., Pirttima, M., et al. (2015). Suberin fatty acids isolated from outer birch bark improve moisture barrier properties of cellulose ether films intended for tablet coatings. *International Journal of Pharmaceutics*, *489*, 91–99.

Heredia, A. (2003). Biophysical and biochemical characteristics of cutin, a plant barrier biopolymer. *Biochimica et Biophysica Acta*, *1620*, 1–7.

Heredia-Guerrero, J. A., Heredia, A., García-Segura, R., & Benítez, J. J. (2009). Synthesis and characterization of a plant cutin mimetic polymer. *Polymer*, *50*, 5633–5637.

Hetzroni, A., Vana, A., & Mizrach, A. (2011). Biomechanical characteristics of tomato fruit peels. *Postharvest Biological Technology*, *59*, 80–84.

Järvinen, R., Kaimainen, M., & Kallio, H. (2010). Cutin composition of selected northern berries and seeds. *Food Chemistry*, *122*, 137–144.

Jiménez, A., Fabra, M. J., Talens, P., & Chiralt, A. (2012). Effect of re-crystallization on tensile, optical and water vapour barriers properties of corn starch films containing fatty acids. *Food Hydrocolloids*, *26*, 302–310.

Kolattukudy, P. E. (1980). Biopolyester membranes of plants: Cutin and suberin. *Science*, *208*, 990–1000.

López-Casado, G., Matas, A. J., Domínguez, E., Cuartero, J., & Heredia, A. (2007). Biomechanics of isolated tomato (*Solanum lycopersicum* L.) fruit cuticles: The role of the cutin matrix and polysaccharides. *Journal of Experimental Botany*, *58*, 3875–3883.

Martin, L. B. B., & Rose, J. K. C. (2014). There's more than one way to skin a fruit: Formation and functions of fruit cuticles. *Journal of Experimental Botany*, *65*, 4639–4651.

Matas, A. J., Cobb, E. D., Bartsch, J. A., Paolillo, D. J., & Niklas, K. J. (2004). Biomechanics and anatomy of *Lycopersicon esculentum* fruit peels and enzyme-treated samples. *American Journal of Botany*, *91*, 352–360.

Monfregola, L., Bugatti, V., Amodeo, P., De Luca, S., & Vittoria, V. (2011). Physical and water sorption properties of chemically modified pectin with an environmentally friendly process. *Biomacromolecules*, *12*, 2311–2318.

Moreira, F. K. V., De Camargo, L. A., Marconcini, J. M., & Mattoso, L. H. C. (2013). Nutraceutically inspired pectin–$Mg(OH)_2$ nanocomposites for bioactive packaging applications. *Journal of Agriculture and Food Chemistry*, *61*, 7110–7119.

OECD. (2017). *Guideline for the testing of chemicals/105/water solubility*. Adopted by the Council on 27th July 1995. Available at:. www.oecd.org/chemicalsafety/risk-assessment/1948185.pdf

Ojagh, S. M., Rezaei, M., Rezavi, S. H., & Hosseini, S. M. H. (2010). Development and evaluation of a novel biodegradable film made from chitosan and cinnamon oil with low affinity toward water. *Food Chemistry*, *122*, 161–166.

Pereda, M., Amica, G., & Marcovich, N. (2012). Development and characterization of edible chitosan/olive oil emulsion films. *Carbohydrate Polymers*, *87*, 1318–1325.

Petracek, P. D., & Bukovac, M. J. (1995). Rheological properties of enzymatically isolated tomato fruit cuticle. *Plant Physiology*, *109*, 675–679.

Pollard, M., Beisson, F., Li, Y., & Ohlrogge, J. B. (2008). Building lipid barriers: Biosynthesis of cutin and suberin. *Trends in Plant Science*, *13*, 136–246.

Rhim, J.-W. (2004). Physical and mechanical properties of water resistant sodium alginate films. *LWT–Food Science and Technology*, *37*, 323–330.

Saha, R., Sarkar, G., Roy, I., Rana, D., Bhattacharyya, A., Adhikari, A., et al. (2016). Studies on methylcellulose/pectin/montmorillonite nanocomposite films and their application possibilities. *Carbohydrate Polymers*, *136*, 1218–1227.

Sartori, T., & Menegalli, F. C. (2016). Development and characterization of unripe banana starch films incorporated with solid lipid microparticles containing ascorbic acid. *Food Hydrocolloids*, *55*, 210–219.